

Helical Hairpin Structure of Influenza Hemagglutinin Fusion Peptide Stabilized by Charge–Dipole Interactions between the N-Terminal Amino Group and the Second Helix

Justin L. Lorieau, John M. Louis, and Ad Bax*

Laboratory of Chemical Physics, National Institute of Diabetes and Digestive and Kidney Diseases, National Institutes of Health, Bethesda, Maryland 20892, United States

S Supporting Information

ABSTRACT: The fusion domain of the influenza coat protein hemagglutinin HA₂, bound to dodecyl phosphocholine micelles, was recently shown to adopt a structure consisting of two antiparallel α -helices, packed in an exceptionally tight hairpin configuration. Four interhelical H ^{α} to C=O aliphatic H-bonds were identified as factors stabilizing this fold. Here, we report evidence for an additional stabilizing force: a strong charge–dipole interaction between the N-terminal Gly¹ amino group and the dipole moment of helix 2. pH titration of the amino-terminal ¹⁵N resonance, using a methylene-TROSY-based 3D NMR experiment, and observation of Gly¹ ¹³C' show a strongly elevated pK = 8.8, considerably higher than expected for an N-terminal amino group in a lipophilic environment. Chemical shifts of three C-terminal carbonyl carbons of helix 2 titrate with the protonation state of Gly¹-N, indicative of a close proximity between the N-terminal amino group and the axis of helix 2, providing an optimal charge–dipole stabilization of the antiparallel hairpin fold. pK values of the side-chain carboxylate groups of Glu¹¹ and Asp¹⁹ are higher by about 1 and 0.5 unit, respectively, than commonly seen for solvent-exposed side chains in water-soluble proteins, indicative of dielectric constants of $\epsilon = \sim 30$ (Glu¹¹) and ~ 60 (Asp¹⁹), placing these groups in the headgroup region of the phospholipid micelle.

The driving force for the formation of the three-dimensional (3D) fold of water-soluble proteins often is dominated by burial of the hydrophobic surfaces of its secondary structure elements, α -helices and β -sheets, which in turn are stabilized by internal H-bonding.¹ In the lipophilic environment of membranes, burial of hydrophobic surfaces does not provide a driving force for stabilizing the tertiary structure of membrane proteins. Instead, electrostatic interactions between elements of secondary structure and aliphatic H-bonds have been proposed as stabilizing factors,² although the magnitude of the energetic contribution of C ^{α} –H \cdots O H-bonds remains a matter of debate.³ Multiple C ^{α} –H \cdots O H-bonds were recently identified in the tight helical hairpin fold of the fusion domain of the HA₂ domain of the influenza virus surface glycoprotein hemagglutinin.⁴ Here, we provide evidence for an additional important stabilizing force resulting from the charge–dipole interaction between the N-terminal NH₃⁺ group of Gly¹ and the dipole moment of helix 2, as evidenced by an elevated pK of the Gly¹ amino group and the impact of its deprotonation on the ¹³C' chemical shifts of C-terminal residues of helix 2. Stabilizing interactions between a helix dipole moment and a positively charged

titratable group have long been recognized to increase the pK value of the titratable group,⁵ and chemical shift changes remote in sequence from the titratable group can provide unambiguous evidence for electrostatic interactions.⁶

Hemagglutinin is solely responsible for mediating the fusion of the viral and the host-cell endosomal membranes during infection.⁷ A ‘spring-loaded’ conformational change of hemagglutinin is triggered by the low pH of the endosome, thereby exposing the N-terminal segment of HA₂.⁸ Following this conformational change, the first 23 residues of HA₂, referred to as HAfp23, become embedded in the target membrane.⁹ HAfp23 is both quite hydrophobic and glycine-rich, and represents the most conserved region of the hemagglutinin protein.¹⁰

Pioneering work by Lear and DeGrado demonstrated that synthetic peptides composed of the first 20 residues of HA₂ (HAfp20) were sufficient to induce fusion of lipid vesicles.¹¹ However, HAfp20, which has been the topic of numerous biophysical and biochemical studies over the past 15 years, lacks the three C-terminal residues, Trp²¹-Tyr²²-Gly²³, which not only are hydrophobic and completely conserved across all serotypes but also interact with the membrane.^{9,12} Moreover, it was recently found that these additional residues significantly impact the tertiary structure of the peptide.⁴ In zwitterionic dodecyl phosphatidylcholine (DPC) micelles, HAfp23 adopts a structure consisting of two α -helices packed together in a very tight helical-hairpin arrangement. Intermolecular NOEs between detergent and HAfp23 indicate that its hydrophobic side faces the core of the detergent micelle, while the more polar side is exposed to solvent,⁴ a conclusion reinforced by paramagnetic relaxation enhancement observed when spin-labeled lipids are added to the detergent (Supporting Information [SI] Figure S1). Two ‘Gly-ridges’, part of a GXXGXXXG and its inverse GXXXGXXG motif, are located at the interhelical interface and enable their very tight packing. We previously identified four interhelical aliphatic C ^{α} H ^{α} \cdots O=C hydrogen bonds, between residue pairs Gly¹/Trp²¹, Ala⁵/Met¹⁷ and Phe⁹/Gly¹³, which are known to stabilize helical packing in membrane proteins.¹³

The HAfp23 structure suggested that the N-terminal amino group of Gly¹ may also form a number of important hydrogen bonds that position its positive charge at the C-terminal end of the peptide's second α -helix, implying a charge–dipole interaction. Together, these interactions may be responsible for the strict conservation of Gly¹ in all serotypes.^{10,14,15} In much of the

Received: November 6, 2010

Published: February 14, 2011

literature, the putative protonation state of Gly¹ has been marked as NH₂, however, and few studies have looked at this topic more closely.¹⁶ Ambiguity regarding the protonation state of Gly¹ has also permeated the molecular modeling literature, where simulations were conducted either for the protonated state,¹⁷ for multiple protonation states,¹⁸ or for an unspecified or deprotonated state.¹⁹

Zhou et al. found a pK of 8.69 for Gly¹ of the truncated fusion peptide,¹⁶ which is elevated compared to values for peptides in solution (pK 7.5–8.0).²⁰ An elevated pK for this N-terminal amino group is surprising, considering that even in aqueous solution the pK value of the N-terminal amino group of an α -helix is depressed by about 0.5 units by the positive potential imposed by the helix dipole moment.²¹ Embedding of the peptide in the hydrophobic environment of neutral membranes would be expected to decrease its pK value even further,^{22,23} but a potential α -NH₃⁺ interaction with one of the carboxyl groups of the peptide or with the phosphate of the lipid headgroup was proposed as a possible reason for the elevated pK of Gly¹.¹⁶ This truncated fusion peptide was subsequently reported to adopt an open ‘boomerang’ structure,²⁴ while embedding its α -NH₃⁺ in the lipid bilayer, without revealing any interactions that could stabilize its protonated state. We recently found that the open boomerang structure of truncated HAfp20, which also contains a C-terminal ‘solubilization tag’, is dynamic and transiently adopts the helical-hairpin structure of HAfp23.⁴ In an effort to evaluate whether stabilizing interactions in this hairpin can account for the elevated pK value, we set out to measure the pK values of titratable groups in full-length HAfp23. Furthermore, we measure pK values of the only two negatively charged side chains in HAfp23 of serotype H1: Glu¹¹ and Asp¹⁹, with Glu¹¹ found to change protonation states at the pH where fusion is activated.

Solution NMR of membrane-binding proteins, usually carried out on detergent-solubilized systems,²⁵ is a powerful approach for obtaining detailed structural information. The protonation state of an amine group is probed most easily by its ¹⁵N chemical shift, which undergoes a substantial \sim 12 ppm upfield change upon deprotonation.²⁶ Hydrogen-exchange rates with solvent of the amino hydrogens of Gly¹ are too high to permit observation of their resonance with a standard ¹⁵N HSQC experiment. In order to avoid ambiguity between the Gly¹ amino group and the side chains of multiple Lys residues in the C-terminal solubilization tag of HAfp23, we probed the Gly¹ ¹⁵N chemical shift indirectly, using a new 3D CH₂-TROSY HACAN experiment, which is particularly well suited for Gly residues (SI, Figure S2). This experiment correlates the ¹⁵N chemical shift of residues *i* and *i* + 1 to the ¹H ^{α} and ¹³C ^{α} chemical shifts of residue *i*, assigned previously.⁴ Gly methylene groups in D₂O solution constitute well-isolated ¹H ^{$\alpha 2$} /¹H ^{$\alpha 3$} /¹³C ^{α} three-spin systems, which can be detected in a resolution- and sensitivity-optimized manner by the CH₂-TROSY scheme.²⁷

The pH dependence of the amino terminal ¹⁵N resonance is readily observed from cross sections through the 3D CH₂-TROSY HACAN spectra (Figure 1A), and fits well to the standard Henderson–Hasselbalch equation (Figure 1B). The ¹⁵N chemical shift moves from 27 ppm (NH₃⁺ form) to 13.6 ppm (NH₂ form) when increasing the pH, while the Gly¹ ¹³C ^{α} chemical shift moves downfield by 2.5 ppm from 44.3 to 46.8 ppm. The best-fit pK from these measurements and those of ¹³C ^{α} shifts on a separate sample (Figure 2) is 8.80 \pm 0.04, a value slightly above that of the truncated peptide in DPC (pK = 8.63; SI Figure S3).

Two factors are known to significantly impact the pK values of titratable moieties that interact with micelles: the surface potential of the micelle and the difference in partitioning between aqueous and apolar membrane environments for the neutral and

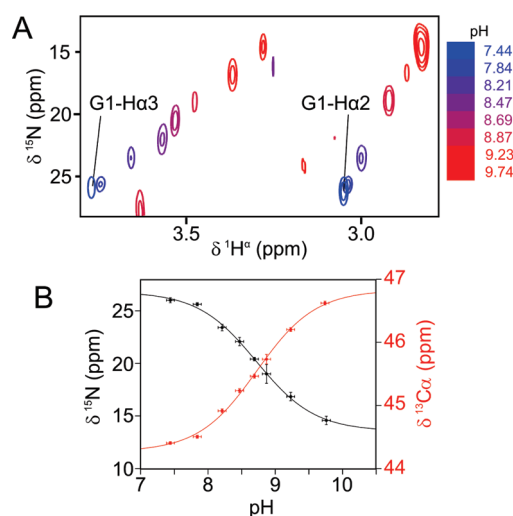


Figure 1. pH titration of the N-terminal amino ¹⁵N resonance of Gly¹ with the HACAN CH₂-TROSY experiment. (A) Superimposed small regions of ¹H/¹⁵N cross sections taken through the 3D CH₂-TROSY HACAN spectrum of HAfp23, showing the correlation between the Gly¹ ¹H ^{$\alpha 2$} /¹H ^{$\alpha 3$} and amino ¹⁵N chemical shifts. (B) The Gly¹ backbone amino ¹⁵N (black) and ¹³C ^{α} (red) chemical shift dependence on pH is shown. A nonlinear least-squares regression was used to fit the Henderson–Hasselbalch equation to the titration curves. The fitted values are: pK = 8.73 \pm 0.07, ¹⁵N and ¹³C ^{α} chemical shifts of 27.0 \pm 0.6 and 44.3 \pm 0.1 ppm, respectively, for the protonated form (NH₃⁺), and 13.6 \pm 0.4 and 46.8 \pm 0.1 ppm, respectively, for the deprotonated form (NH₂). The fitted pK value when measuring the Gly¹ ¹³C ^{α} shift on a separate sample (Figure 2) is 8.84 \pm 0.05.

charged forms of the titratable group.²⁸ The first factor is particularly pertinent for charged micelles and membranes, as illustrated by the increased pK of the α -NH₃ group of the M13 coat protein in anionic micelles.²⁹ The second factor accounts for the high energy associated with burial of charged groups and the stabilization of neutralized species in membranes. Thus, compared to being immersed in water, the population of the charged form of a titratable group will be disfavored in a medium of moderate dielectric constant, ϵ , found at the lipid–water interface or the even lower ϵ in the aliphatic core of the micelle.²⁸

Literature values for the N-terminal amino group pK values of peptides and proteins in free aqueous solution mostly fall in the 7.5–8.0 range.²⁰ In a neutral micelle environment, the pK for the amino group of Gly¹ would be expected to shift toward lower values because the charged NH₃⁺ species is destabilized relative to the neutral NH₂ species in the membrane. For example, for a somatostatin analogue peptide, an amino-terminal pK shift of -0.55 units was observed between bulk solution and binding to a neutral bilayer surface.²³ Accordingly, based solely on the lipid-binding induced pK shift caused by the low-dielectric micelle environment, a pK value lower than \sim 7.5 is expected for Gly¹. The observed Gly¹ pK of 8.80 is higher by at least 0.7 pH units than values expected in aqueous solution; the difference is even greater when the expected destabilization of NH₃⁺ in the decreased dielectric environment of the micelle is taken into account, or the additional increase expected for its location at the N-terminus of an α -helix.²¹ An increase in the pK by one pH unit is indicative of an interaction that stabilizes the NH₃⁺ form by 1.4 kcal/mol; the increase by at least 1.5 pH units therefore corresponds to a stabilization by \sim 2 kcal/mol.

In the absence of an observable ¹H NMR signal for the N-terminal amino group, its potential interaction partners previously could only be inferred from the approximate position of the NH₃⁺ group,

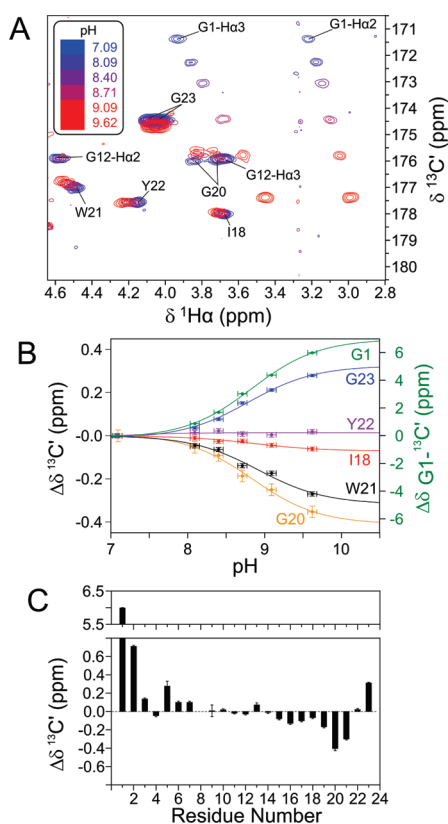


Figure 2. Changes in the $^{13}\text{C}'$ chemical shifts on titrating the amino group of Gly¹. (A) Superimposed small regions of cross sections taken through the 3D HCACO spectra of HAfp23, recorded at pH values ranging from pH 7.09 to 9.62, with $^{13}\text{C}'$ chemical shift changes summarized in (C). The Gly⁸ $^{13}\text{C}'$ chemical shifts could not be identified uniquely due to spectral congestion and are not reported. (B) pH dependence of Gly¹ $^{13}\text{C}'$ (green, right axis) and $^{13}\text{C}'$ chemical shifts of various residues near the end of helix 2. Reported chemical shift changes are relative to values measured at pH 7.09. Traces shown represent nonlinear regression fits to the Henderson–Hasselbalch equation, yielding: $\Delta\delta = 7.1 \pm 0.2$ ppm and $\text{pK} = 8.84 \pm 0.05$ for Gly¹; $\Delta\delta = -0.08 \pm 0.02$ ppm and $\text{pK} = 8.9 \pm 0.2$ for Ile¹⁸; $\Delta\delta = -0.46 \pm 0.02$ ppm and $\text{pK} = 8.84 \pm 0.09$ for Gly²⁰; $\Delta\delta = -0.35 \pm 0.06$ ppm and $\text{pK} = 8.9 \pm 0.2$ for Trp²¹; $\Delta\delta = +0.37 \pm 0.04$ ppm and $\text{pK} = 8.87 \pm 0.10$ for Gly²³.

calculated without its stabilizing restraints.⁴ However, pH titration allows for straightforward evaluation of potential interaction partners, which are expected to be significantly impacted by a change in protonation state of the amino group. As can be seen (Figure 2), besides upfield changes in the chemical shifts of Gly¹, Leu², and Ala⁵ $^{13}\text{C}'$ located proximate to the N-terminal amino group, substantial changes are also observed for Gly²⁰, Trp²¹, and Gly²³ carbonyl resonances, pointing to potential H-bonds to the Gly¹ amino protons. The pH values corresponding to the midpoints of the chemical shift change observed for these C-terminal carbonyl resonances (Figure 2B) match those of Gly¹, which further substantiates a connection between these groups. Indeed, such interactions are geometrically allowed, and would stabilize the observed tight antiparallel packing of the two helices. Moreover, H-bonding of the three amino protons to Gly²⁰, Trp²¹, and Gly²³ carbonyl oxygens positions the positively charged amino group close to the center of helix 2, resulting in a favorable interaction with the dipole moment of this helix, rather than the unfavorable charge–dipole interaction that would occur if the NH_3^+ were positioned on the helix 1 axis. A small

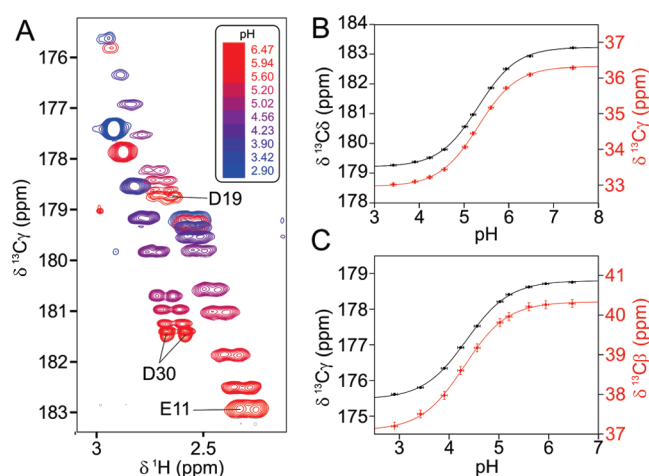


Figure 3. Chemical shift titrations of the carboxylate groups of Glu¹¹ and Asp¹⁹. (A) Superimposed small regions of cross sections taken through the 3D HCCO spectra taken over the pH range 6.5–2.9, showing the correlation between the carboxylic acid ^{13}C and its vicinal methylene ^1H chemical shifts. Chemical shift versus pH for (B) the Glu¹¹ side chain $^{13}\text{C}^\delta$ (black) and $^{13}\text{C}^\gamma$ (red), and (C) the Asp¹⁹ side chain $^{13}\text{C}^\gamma$ (black) and $^{13}\text{C}^\beta$ (red) are fit to the Henderson–Hasselbalch equation using nonlinear least-squares regression. Fitted values for (B) are: $\text{pK} = 5.31 \pm 0.01$, with $^{13}\text{C}^\delta$ and $^{13}\text{C}^\gamma$ chemical shift of 179.2 ppm and 33.0 ppm, respectively, for the protonated form (COOH), and $^{13}\text{C}^\delta$ and $^{13}\text{C}^\gamma$ chemical shifts of 183.2 and 36.3 ppm, respectively, for the deprotonated form (COO^-). Fitted values for Asp¹⁹ are $\text{pK} = 4.35 \pm 0.02$, with $^{13}\text{C}^\gamma$ and $^{13}\text{C}^\beta$ chemical shift of 175.5 and 37.1 ppm, respectively, for the protonated form, and $^{13}\text{C}^\gamma$ and $^{13}\text{C}^\beta$ chemical shifts of 178.8 and 40.3 ppm for the deprotonated form (COO^-).

impact (0.1–0.2 ppm $^{13}\text{C}'$ upfield shift) of the deprotonation of Gly¹ is also seen for the three carbonyls (Gly¹⁶, Met¹⁷, and Asp¹⁹) that make α -helical H-bonds to these carboxy-terminal residues. Even though a weakening of an H-bond is known to be associated with an upfield $^{13}\text{C}'$ shift, it should be noted that quantitative interpretation of the observed $^{13}\text{C}'$ shift changes is difficult, because the loss of an intramolecular H-bond to a carbonyl oxygen almost certainly will be replaced by an H-bond to a water molecule or to a choline headgroup of DPC, with an interaction strength and impact on the $^{13}\text{C}'$ shift that is difficult to calculate quantitatively.

Further evidence for destabilization of the helical hairpin structure at high pH can be found in the $^{13}\text{C}^\alpha$ chemical shift changes that occur upon deprotonation of Gly¹- NH_3^+ . These changes correlate fairly well with the $^{13}\text{C}^\alpha$ chemical shift difference seen between the tightly folded HAfp23 sequence at pH 7.4, and $^{13}\text{C}^\alpha$ chemical shifts observed for a G8A mutant, designed to disrupt the tight antiparallel packing of the two helices (Figure S4 in SI). Interestingly, the spectral data observed for G8A also correlate well with those of the truncated HAfp20 fusion peptide (data not shown), which presumably is destabilized because it lacks the three helical C-terminal residues found to interact with the Gly¹ amino group in HAfp23.

Titration plots for Glu¹¹ and Asp¹⁹ show that ^{13}C chemical shifts move upfield as the carboxylates are protonated by 3.3 ppm for Glu¹¹, and by 3.2 ppm for Asp¹⁹ (Figure 3). A nonlinear fit of the titrations to the Henderson–Hasselbalch equation yields pK values of 5.31 for Glu¹¹ and 4.35 for Asp¹⁹. A satisfactory fit was achieved without recourse to a Hill coefficient. Compared to model pentapeptides, which have side-chain pK values of 4.25 ± 0.05 (Glu) and 3.90 ± 0.02 (Asp),²¹ the pK values in HAfp23 are higher by 1.1 (Glu¹¹) and 0.5 (Asp¹⁹) units.

In the absence of stabilizing interactions, a shift in pK can be attributed to the decreased local dielectric constant near the titratable group, resulting from its location with respect to the water lipid interface. For small indicator molecules, a one unit change in pK between water and a neutral micelle solution has been translated into a shift from $\epsilon = 80$ to $\epsilon = 32$.²⁸ pK values we find for the side chain carboxylate groups of Glu¹¹ and Asp¹⁹ are higher by about 1 and 0.5 unit, respectively, than commonly seen for short reference peptides in water, and if these changes are attributed to the change in dielectric constant for the neutral DPC micelle, one similarly obtains $\epsilon \approx 30$ for Glu¹¹, and $\epsilon \approx 60$ for Asp¹⁹, which places these side-chain carboxylates in the headgroup region.

A previous study of the 25-residue H3 subtype fusion peptide in SDS micelles reported pK values for Glu¹¹, Glu¹⁵ and Asp¹⁹ of 5.91, 5.25, and 5.19, respectively.³⁰ These pK values in negative micelles are 0.6–0.8 units higher than those found by us in neutral micelles, an effect that may be attributed to the negative charge of the SDS sulfate head-groups, giving rise to a strong negative surface potential for the micelle, which further destabilizes the negatively charged carboxylate state. The increase in pK between charged and neutral micelles can be quite significant; a pK increase as high as +2.3 has been observed between species bound to neutral and negatively charged micelles.²⁸

The functional roles of Glu¹¹ and Asp¹⁹ in the fusion peptide are not entirely clear. Serotypes with Ala and Asn substitutions for Asp¹⁹ also occur,¹⁰ while Glu¹¹ is strictly conserved. However, hemagglutinin protein with an E11V mutation is fusogenic and shows no change in the optimal pH of 5.5 for fusion.¹⁵ Interestingly, however, the pK of Glu¹¹ coincides with this optimal pH of fusion, and even though the monomeric structure of HAfp23 does not change significantly between pH 4.0 and 7.4,⁴ the protonated state of Glu¹¹ may be required for switching to the postulated oligomeric structure required for actual fusion.

■ ASSOCIATED CONTENT

Supporting Information. Experimental details and analyses. This material is available free of charge via the Internet at <http://pubs.acs.org>.

■ AUTHOR INFORMATION

Corresponding Author

bax@nih.gov

■ ACKNOWLEDGMENT

This work was supported by the Intramural Research Program of the NIDDK, NIH, and by the Intramural Antiviral Target Program of the Office of the Director, NIH. We thank Dennis A. Torchia for useful discussions.

■ REFERENCES

- (1) Creighton, T. E. *Proteins: Structures and Molecular Properties*; Macmillan: New York, 1993.
- (2) Senes, A.; Ubarretxena-Belandia, I.; Engelman, D. M. *Proc. Natl. Acad. Sci. U.S.A.* **2001**, *98*, 9056–9061.
- (3) Yohannan, S.; Faham, S.; Yang, D.; Grosfeld, D.; Chamberlain, A. K.; Bowie, J. U. *J. Am. Chem. Soc.* **2004**, *126*, 2284–2285.
- (4) Lorieau, J. L.; Louis, J. M.; Bax, A. *Proc. Natl. Acad. Sci. U.S.A.* **2010**, *107*, 11341–11346.
- (5) Perutz, M. F.; Gronenborn, A. M.; Clore, G. M.; Fogg, J. H.; Shih, D. T. B. *J. Mol. Biol.* **1985**, *183*, 491–498. Sali, D.; Bycroft, M.; Fersht, A. R. *Nature* **1988**, *335*, 740–743.
- (6) Tomlinson, J. H.; Ullah, S.; Hansen, P. E.; Williamson, M. P. *J. Am. Chem. Soc.* **2009**, *131*, 4674–4684.

- (7) Wiley, D. C.; Skehel, J. J. *Annu. Rev. Biochem.* **1987**, *56*, 365–394.
- (8) Carr, C. M.; Chaudhry, C.; Kim, P. S. *Proc. Natl. Acad. Sci. U.S.A.* **1997**, *94*, 14306–14313. Cross, K. J.; Langley, W. A.; Russell, R. J.; Skehel, J. J.; Steinhauer, D. A. *Protein Pept. Lett.* **2009**, *16*, 766–778.
- (9) Durrer, P.; Galli, C.; Hoenke, S.; Corti, C.; Gluck, R.; Vorherr, T.; Brunner, J. *J. Biol. Chem.* **1996**, *271*, 13417–13421.
- (10) Nobusawa, E.; Aoyama, T.; Kato, H.; Suzuki, Y.; Tateno, Y.; Nakajima, K. *Virology* **1991**, *182*, 475–485.
- (11) Lear, J. D.; Degrado, W. F. *J. Biol. Chem.* **1987**, *262*, 6500–6505.
- (12) Gray, C.; Tatulian, S. A.; Wharton, S. A.; Tamm, L. K. *Biophys. J.* **1996**, *70*, 2275–2286. Dubovskii, P. V.; Zhmak, M. N.; Maksae, G. I.; Arseniev, A. S. *Russ. J. Bioorg. Chem.* **2004**, *30*, 196–198.
- (13) MacKenzie, K. R.; Prestegard, J. H.; Engelman, D. M. *Science* **1997**, *276*, 131–133. Russ, W. P.; Engelman, D. M. *J. Mol. Biol.* **2000**, *296*, 911–919. Kleiger, G.; Grothe, R.; Mallick, P.; Eisenberg, D. *Biochemistry* **2002**, *41*, 5990–5997.
- (14) Gething, M. J.; Doms, R. W.; York, D.; White, J. J. *Cell Biol.* **1986**, *102*, 11–23. Wu, C. W.; Cheng, S. F.; Huang, W. N.; Trivedi, V. D.; Veeramuthu, B.; Kantchev, A. B.; Wu, W. G.; Chang, D. K. *Biochim. Biophys. Acta* **2003**, *1612*, 41–51.
- (15) Steinhauer, D. A.; Wharton, S. A.; Skehel, J. J.; Wiley, D. C. *J. Virol.* **1995**, *69*, 6643–6651.
- (16) Zhou, Z.; Macosko, J. C.; Hughes, D. W.; Sayer, B. G.; Hawes, J.; Epan, R. M. *Biophys. J.* **2000**, *78*, 2418–2425.
- (17) Spassov, V. Z.; Yan, L.; Szalma, S. *J. Phys. Chem. B* **2002**, *106*, 8726–8738.
- (18) Huang, Q.; Chen, C. L.; Herrmann, A. *Biophys. J.* **2004**, *87*, 14–22. Sammalkorpi, M.; Lazaridis, T. *Biochim. Biophys. Acta* **2007**, *1768*, 30–38. Panahi, A.; Feig, M. *J. Phys. Chem. B* **2010**, *114*, 1407–1416.
- (19) Sammalkorpi, M.; Lazaridis, T. *Biophys. J.* **2007**, *92*, 10–22. Lague, P.; Roux, B.; Pastor, R. W. *J. Mol. Biol.* **2005**, *354*, 1129–1141. Vaccaro, L.; Cross, K. J.; Kleinjung, J.; Straus, S. K.; Thomas, D. J.; Wharton, S. A.; Skehel, J. J.; Fraternali, F. *Biophys. J.* **2005**, *88*, 25–36. Jang, H.; Michaud-Agrawal, N.; Johnston, J. M.; Woolf, T. B. *Proteins: Struct., Funct., Bioinf.* **2008**, *72*, 299–312. Li, J. Y.; Das, P.; Zhou, R. H. *J. Phys. Chem. B* **2010**, *114*, 8799–8806. Kasson, P. M.; Lindahl, E.; Pande, V. S. *PLoS Comput. Biol.* **2010**, *6*, 1137–1147.
- (20) Nozaki, Y.; Tanford, C. *Methods Enzymol.* **1967**, *11*, 715–734. Thurlkill, R. L.; Grimsley, G. R.; Scholtz, J. M.; Pace, C. N. *Protein Sci.* **2006**, *15*, 1214–1218.
- (21) Lockhart, D. J.; Kim, P. S. *Science* **1993**, *260*, 198–202. Sitkoff, D.; Lockhart, D. J.; Sharp, K. A.; Honig, B. *Biophys. J.* **1994**, *67*, 2251–2260.
- (22) Woolley, G.; Deber, C. *Biopolymers* **1987**, *26*, S109–S121.
- (23) Beschiaschvili, G.; Seelig, J. *Biochemistry* **1992**, *31*, 10044–10053.
- (24) Han, X.; Bushweller, J. H.; Cafiso, D. S.; Tamm, L. K. *Nat. Struct. Biol.* **2001**, *8*, 715–720.
- (25) Opella, S. J.; Marassi, F. M. *Chem. Rev.* **2004**, *104*, 3587–3606. Krueger-Koplin, R. D.; Sorgen, P. L.; Krueger-Koplin, S. T.; Rivera-Torres, A. O.; Cahill, S. M.; Hicks, D. B.; Grinius, L.; Krulwich, T. A.; Girvin, M. E. *J. Biomol. NMR* **2004**, *28*, 43–57. Van Horn, W. D.; Kim, H. J.; Ellis, C. D.; Hadziselimovic, A.; Sulistijo, E. S.; Karra, M. D.; Tian, C. L.; Sonnichsen, F. D.; Sanders, C. R. *Science* **2009**, *324*, 1726–1729.
- (26) Zhu, L. Y.; Kemple, M. D.; Yuan, P.; Prendergast, F. G. *Biochemistry* **1995**, *34*, 13196–13202.
- (27) Miclet, E.; Williams, D. C.; Clore, G. M.; Bryce, D. L.; Boisbouvier, J.; Bax, A. *J. Am. Chem. Soc.* **2004**, *126*, 10560–10570.
- (28) Fernandez, M. S.; Fromherz, P. *J. Phys. Chem.* **1977**, *81*, 1755–1761.
- (29) Henry, G. D.; Weiner, J. H.; Sykes, B. D. *Biochemistry* **1986**, *25*, 590–598.
- (30) Chang, D. K.; Cheng, S. F.; Lin, C. H.; Kantchev, E. A. B.; Wu, C. W. *Biochim. Biophys. Acta* **2005**, *1712*, 37–51.